Characterization of glioma cell line characteristics via antibody labeling in an orthotopic zebrafish model

Undergraduate Research Thesis

Presented in Partial Fulfillment of the Requirements for graduation "with Honors Research Distinction in Neuroscience" in the undergraduate colleges of The Ohio State University

by
Brian Jaros

The Ohio State University
April 2016

Project Advisor: Dr. Christine Beattie, Department of Neuroscience

Abstract

Glioblastoma (GBM) is a highly aggressive form of brain cancer with limited efficacious treatments and thus a low survival time in patients. To further understand the biology of GBM tumors, we utilized immunohistochemistry in an orthotopic xenotransplantation model of GBM in zebrafish. Patient-derived GBM cells were cultured and transplanted into larval animals to recapitulate the disease. Two cell types, GBM9 neurospheres and adherent cells, were characterized using markers of proliferation, differentiation, and stemness. Adherent cells were found to express higher levels of proliferation compared to neurospheres. While adherent cells displayed high levels of vimentin and glial fibrillary acidic protein (GFAP) at all time points, neurospheres expressed low levels of these markers early on that increased significantly over time *in vivo*. Conversely, neurospheres expressed high levels of Sox-2 positive cells early on with these populations decreasing over time. Adherent cells displayed low levels of Sox-2 positive cells over time, consistent with the static nature seen in GFAP and vimentin expression and opposite to the dynamic nature of neurospheres. Simultaneous labeling of multiple markers was utilized to further understand the relationship between the division rates of different cell populations. A small population of differentiated vimentin positive neurospheres was found to be dividing at a 5 dpt, while a majority of sox-2 positive neurospheres were dividing at the same time point. The number of dividing stem cells increased over time. Early on, a majority of GFAP positive cells were found to be proliferating but this number decreased significantly by 10 dpt. The results provide a deeper understanding of the biology of GBM tumors, specifically in relation to characteristics displayed by patient tumors.

Introduction

Glioblastoma (GBM) is an aggressive type of brain cancer with a poor prognosis in patients. The incidence rate of the disease is 3.19 per 100,000 individuals and has the highest malignancy rate of all types of primary brain and spinal cord tumors (Ostrom et al., 2014). Modern treatment options for GBM are limited, but include surgical resection followed by radiation and chemotherapy, typically with temozolomide which acts via DNA alkylation (Welker et al., 2016). According to the American Brain Tumor Association, the median survival for patients with combined chemotherapeutic and radiation therapy is roughly 14.6 months. Additionally, only about 10% of patients receiving such concurrent therapies survived beyond a 5 year time points (Stupp et al., 2009). Despite administration of these therapeutic methods, tumor reoccurrence almost always occurs. The deadliness of glioblastoma, combined with the lack of efficacious therapy options, clearly demonstrates a need for a better understanding of the disease to produce enhanced clinical outcomes for patients.

Currently, murine models are commonly used to study glioblastoma. These models are typically either xenotransplant models or genetic models (GEMs). In the xenotransplant method, cells from or derived from a human tumor are transplanted into the animal to produce a tumor. In the genetic model, oncogenes are manipulated and altered so that the animal begins to form cancer cells, and then tumors, on its own. Xenograft mouse models have been used to study the use of the primary chemotherapeutic agent, Temozolomide, in bioluminescent glioblastoma (Dinca et al., 2007). These xenotransplant models are strong since they use patient-derived cells, and thus more closely represent human tumors (Richmond & Su, 2008). However, xenotransplanation into the mouse requires the animal to be artificially immunocompromised so that the host's immune system does not eliminate the cells, preventing the formation of a tumor.

In addition, live imaging is a significant drawback to the murine model. Magnetic resonance imaging and bioluminescence are the primary methods used to visualize tumors in live animals. Both of these forms of imaging are expensive, time-consuming, and provide poor cellular resolution. To examine tumors at a detailed cellular level, animals must be sacrificed and sectioned. Ultimately, these drawbacks in live imaging result in a compromised ability to understand tumor cell behavior and activity in the same animal over time. Furthermore, the time-consuming and low cellular resolution of live-imaging leads large-scale drug investigations to be inefficient in the murine GBM model.

Due to the drawbacks of the murine model, our laboratory selected zebrafish as the model organism for GBM. Zebrafish have become notable model organisms for many human diseases, both developmental and genetic (Dooley & Zon, 2000). This vertebrate organism harbors many advantages including high progeny numbers, inexpensive maintenance, an ability to be genetically manipulated, easy examination of developmental processes, and the capacity for high-output genetic screens. The zebrafish has more recently emerged as a model for different types of cancer investigation including liver, ocular, and skin cancers, as well as blood (leukemia) and muscle (rhabdomyosarcoma) cancers (Feitsma & Cuppen, 2008). In fact, glioma has also been previously studied in zebrafish, particularly through xenotransplantation (Vittori et al., 2015). Yang et al, 2013 studied the effects of glioma on local angiogenesis using transplantation of red fluorescent glioma cells into the yolk of zebrafish and showed the responsiveness of blood vessel invasion to therapeutic agents. In addition to the injection of glioma cells into the yolk, groups have also transplanted glioma cells directly into the brain of the zebrafish. Lal et al. (2011) showed that certain signals, such as calpain 2, are required for transplanted glioma cells to migrate within the microenvironment of the brain. Kitambi et al.

(2014) screened transplanted adherent glioma cells for vulnerability to over 200 potential targeted treatments. Despite these advances, no study had been performed to carefully characterize and standardize glioma cell behavior in the zebrafish brain to ask how these tumors develop.

To generate a standardized zebrafish GBM model, our laboratory injected cultured, patient-derived GBM cells into the midbrain-hindbrain boundary of zebrafish at 30-36 hours post fertilization. In our model, a specific line of *casper* mutant zebrafish were utilized. These mutants lack pigment in their scales and fins which allows fluorescent tumors to be imaged in live animals under a spinning disk confocal microscope. This type of imaging is both efficient and inexpensive and provides high cellular resolution in the visualization of tumors in live animals, a characteristic not available in the murine model. Due to these live imaging capabilities in *casper* zebrafish, as well as their small size and their ability to absorb chemical compounds in their aquatic environment, the zebrafish is a strong candidate for high-output screening of novel cancer drug compounds. For example, zebrafish were utilized in the discovery of a COX-2 inhibitor as a potential treatment in a zebrafish model of leukemia (Peal, Peterson, & Milan, 2010). Additionally, larval zebrafish were utilized for our model. Because zebrafish do not have an adaptive immune system during the first three weeks of life, utilizing animals in this time frame dissipated a need for immunocompromising zebrafish prior to xenotransplantation. Because of the imaging capabilities of the *casper* mutants, we were able to image fluorescent tumors in live animals were able to be imaged over time using confocal microscopy. From 2 days post transplant to 10 days post transplant, an increase in the volume and spread of tumor cells was observed.

Here, we use histoimmunochemistry to characterize the biology of xenotransplanted glioma tumors, specifically in comparison to the composition of human tumors. In our first set of experiments, we compare two GBM cell types, adherent cells (X12 line) and neurospheres (GBM9 line) *in vivo*. In order to characterize the tumors, we utilized clinical markers, including Ki67, proliferating cell nuclear antigen (PCNA), vimentin, Sox-2, and glial fibrillary acidic protein (GFAP). We demonstrate that X12 adherent cells and GBM9 neurospheres both exhibit markers of proliferation, differentiation, and stem-cell populations. However, adherent cells and neurospheres displayed different levels of cellular markers at different time points, with neurosphere expression being dynamic throughout tumor growth and adherent cell expression remaining relatively constant. In our second set of experiments, double labeling techniques were utilized to understand the relationship between division and the expression of other cell markers. We show that although overall division remains constant in neurospheres over time, the division rates of specific cell populations changes.

Results

Immunohistological labeling reveals that GBM9 cells are more dynamic than X12 adherent cells *in vivo*

In order to better understand the biological makeup of glioblastoma tumors, two cell types, GBM9 neurospheres and X12 adherent cells, were evaluated using immunohistochemistry. Although neurospheres and adherent cells have been described in depth in *in vitro*, a direct comparison of how these tumor cells developed in an *in vivo* environment has not been performed in any animal model system to the best of our knowledge. Neurospheres were originally developed to both expand and isolate neural stem cells *in vitro* (Rahman et al.,

2015). In a general neurosphere assay, cells derived from patient tumors are cultured in a serum-free medium to which growth factors are added in order to promote the propagation of progenitor cells resulting in the formation of the characteristic sphere shape (Rahman et al., 2015). Conversely, adherent cells are grown on culture that has been treated with serum which specifically permits cell adhesion (ThermoFisher Scientific). Both lines were patient-derived, cultured, and transfected to express green fluorescent protein (GFP), which is used for their identification throughout our experiments.

GBM9 neurospheres steadily divide while X12 adherent cells show an increase in proliferation over time

To address whether adherent versus neurosphere glioblastoma cell lines behaved differently *in vivo*, we began by analyzing cell division using the proliferation marker Ki67. Patient glioblastoma tumors exhibit variability in proliferation expression, with one study finding a mean proliferation heterogeneity of 23.8% as defined by Ki67 labeling (Jakovlevs et al, 2014). In fact, it was found that higher levels of tumor proliferation, as measured by Ki67 positive cells, were correlated with shorter recurrence-free time intervals (Schroder et al, 2002). As tumor recurrence is a significant, contributing factor to patient mortality, the evaluation of Ki67 in the animal tumors is extremely clinically relevant and may be related to prognostic outcome. In addition, current chemotherapeutic treatments, such as Temozolomide, target dividing cells. Thus, an understanding of tumor cell proliferation is relevant to patient treatment and outcome.

We found that both X12 adherent cells and GBM9 neurospheres were proliferating as indicated by observation of Ki67 positive tumor cells. The presence of dividing cells aligned with a previous observation from our lab that tumor burden, as measured by volume, increased

over time (Welker et al., 2016). Although both types of tumor cells were positive for the marker, they differed in their expression at various time points. GBM9 neurospheres were found to remain relatively constant throughout the 2, 5, and 10 day time points with a slight increase over time. The mean percentage of Ki67 positive cells was ~43% and was not significantly different between times. Conversely, the proliferation of X12 adherent cells was comparable to that of the neurospheres at 2 dpt (~50%), but increase markedly over the 5 and 10 day time points (~69%). Additionally, it was found that the number of Ki67+ cells in X12 tumors was significantly higher at 10 dpt, perhaps due to the larger amount of cells in the tumors. Therefore, similar to patient tumors, both adherent and neurosphere derived tumors contain proliferating cells.

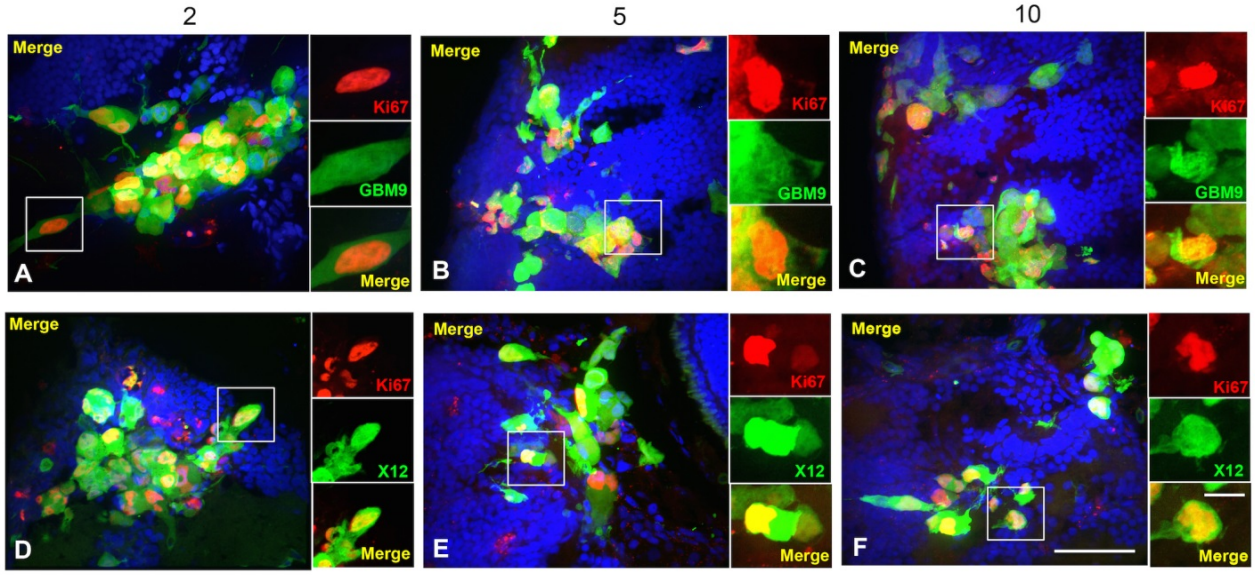

GBM9 neurospheres steadily divide while X12 adherent cells show an increase in proliferation over time

Confocal images of GBM9 and X12 on 2 (A,D), 5 (B,E) and 10 (C,F) dpt transverse cryosections. (A-C) GBM9 (green), DAPI (blue) and Ki67 (red) at 100×. (D-F) X12 (green), DAPI (blue) and Ki67 (red) at 100×. White boxes denote magnified area to the right of the image. *n*=5 animals per group; 30 animals total. Scale bar: 20 μm for main panels and 5 μm for insets.

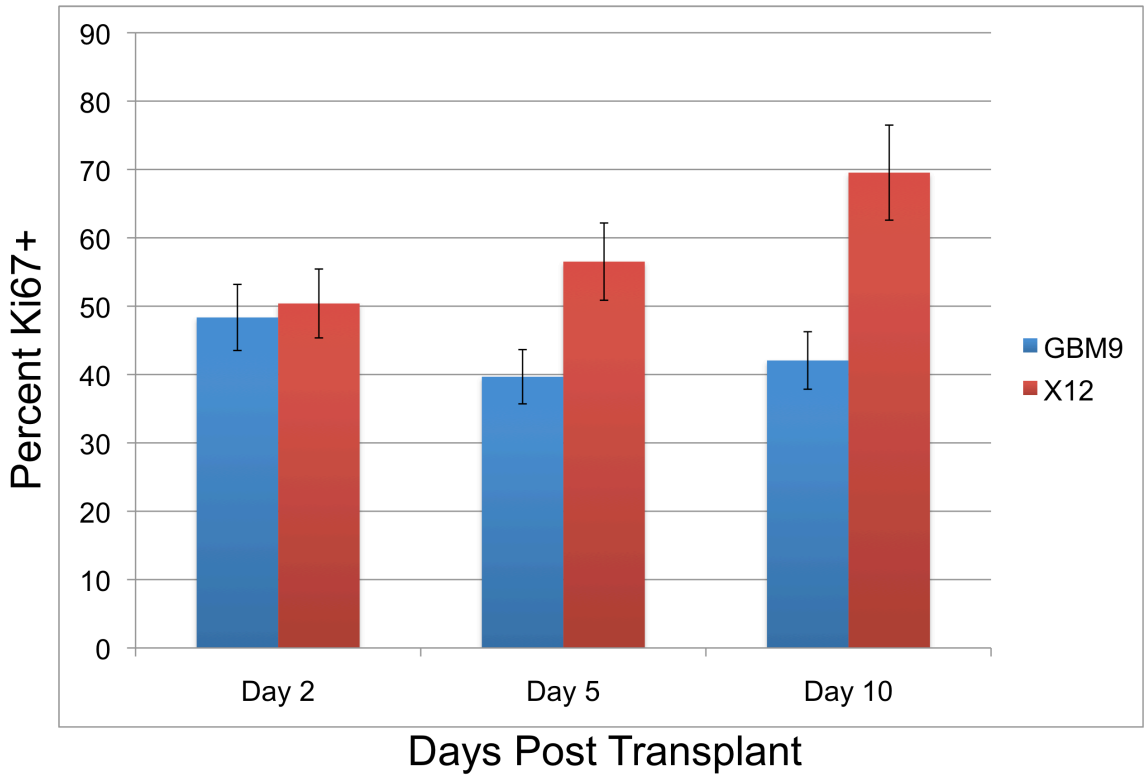

Quantification of the percentage of dividing tumors cells at each time point for GBM9 (blue bar) and X12 (red bar) transplants.

GBM9 neurospheres differentiate over time while X12 adherent cells express high differentiation markers at both early and late time points

Next, we analyzed the differentiation of tumor cells using vimentin and glial fibrillary acidic protein (GFAP) markers. Vimentin is a protein that makes up the intermediate filaments of the cytoskeleton of cells, particularly when they are in the mesenchymal state. Although expressed in healthy human cells, vimentin is found to be overexpressed in many types of cancer, including tumors of the central nervous system (Satelli et al., 2011). This heightened level of expression is correlated with more aggressive tumors that display increased growth and invasion leading to decreased patient survival (Satelli et al., 2011). In fact, vimentin was found to be a key mediator of malignancy in glioblastoma, working as part of the integrin trafficking pathway which can be activated by galectin-1 (Fortin et al., 2010). Levels of vimentin expression

in glioma cells were found to vary based on factors such as cell density, therapeutic treatment, and tumor region, with low-density tumors in migrated regions experiencing increased expression following constant temozolomide treatment (Trog et al., 2008). Due to its presence in many types of cancer, including glioma, its heterogeneity among tumor cells, and its correlations with factors related to patient prognosis, there is a strong clinical relevance to our investigation of vimentin as a glioblastoma marker.

At 2 dpt, a very low number of GBM9 neurospheres were found to be positive for vimentin expression. This suggests that at this early time point, these neurospheres are undifferentiated and are not in a mesenchymal state. At the 5 and 10 day time point, the number of GBM9 neurospheres expressing vimentin increased significantly to nearly ~95% suggesting that these cells are differentiating and assuming a mesenchymal state over time *in vivo*. Conversely, X12 adherent cells were found to have high levels of vimentin expression throughout the time frame examined (2, 5, and 10 dpt). The number of vimentin positive X12 cells increased slightly over time (~76% - 91%), but high levels at the 2 day time point suggest that these adherent cell derived tumors are largely differentiated upon transplantation. These results show that both glioma cell lines express high levels of vimentin, similar to the overexpression reported in human tumors, although adherent cells and neurospheres display different expression levels with neurospheres showing a more dynamic increase in vimentin over time *in vivo*.

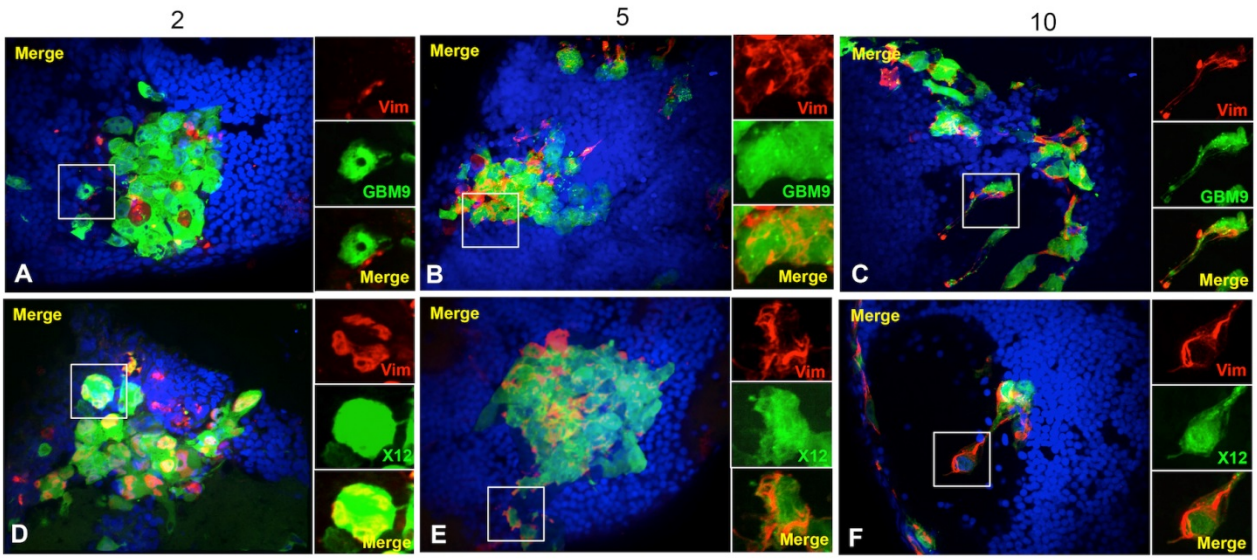

GBM9 neurospheres differentiate over time while X12 adherent cells express high differentiation markers at both early and late time points

Confocal images of GBM9 and X12 on 2 (A,D), 5 (B,E) and 10 (C,F) dpt transverse cryosections. (A-C) GBM9 (green), DAPI (blue) and vimentin (red) at 100×. (D-F) X12 (green), DAPI (blue) and vimentin (red) at 100×. White boxes denote magnified area to the right of the image. *n*=5 animals per group; 30 animals total. Scale bar: 20 μm for main panels and 5 μm for insets.

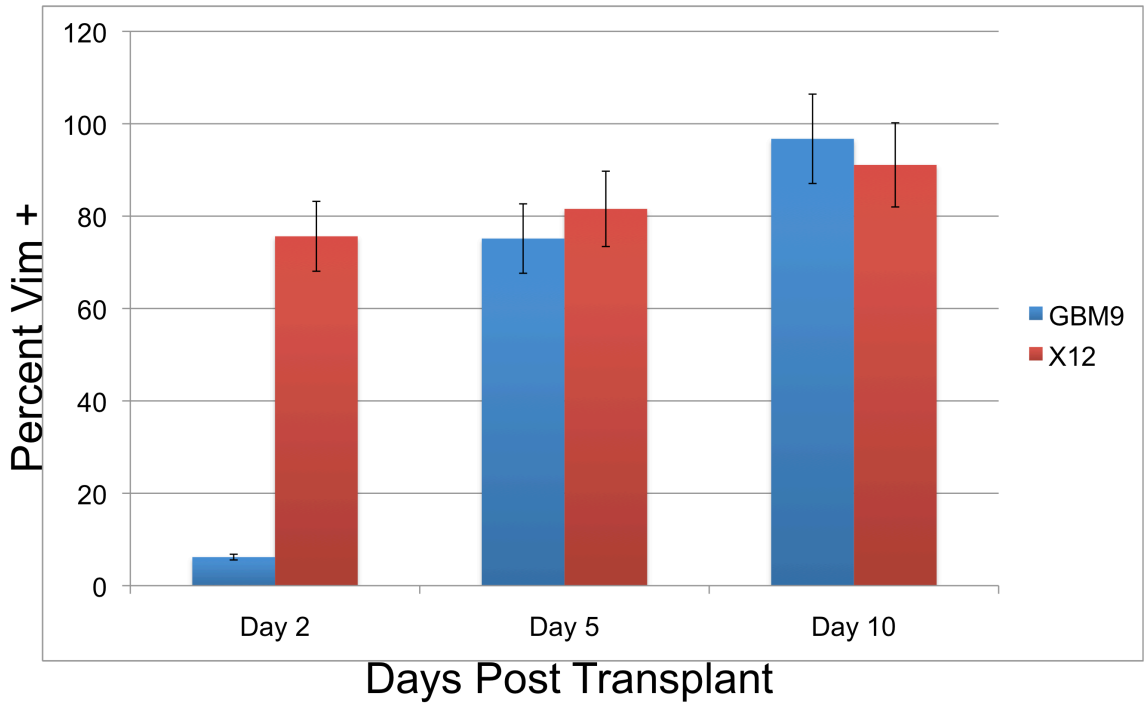

Quantification of the percentage of tumors cells expressing vimentin at each time point for GBM9 (blue bar) and X12 (red bar) transplants.

As mentioned, we also analyzed expression of glial fibrillary expression protein (GFAP) as a marker of differentiation. GFAP is a protein found throughout the human nervous system, notably in glial support cells of the central nervous system such as astrocytes and ependymal cells. Clinically, increased serum GFAP levels have been found to be a useful diagnostic indicator of glioblastoma, specifically in differentiating the disease from other low-grade gliomas (Jung et al., 2007). In fact, increased levels of GFAP were correlated with pathological characteristics such as tumor volume and tumor necrosis volume as evaluated by magnetic resonance imaging. (Jung et al., 2007). Thus, our examination of GFAP is relevant to current clinical and mechanistic investigations of glioma.

We found that GFAP to paralleled that of vimentin, in accordance with their similar indications of differentiation. Early on (2 dpt), only ~3% of GBM9 neurospheres were found to be GFAP+. The expression of GFAP in GBM9 neurospheres was dynamic and found to increase significantly over time (~38% at 5 dpt and ~82% at 10 dpt) suggesting development and differentiation of these tumors *in vivo*. Conversely, a consistent number of X12 adherent cells (~94%) were found to express GFAP at all 3 times points. Again, these results suggest that neurospheres and adherent cells display different characteristics *in vivo* but both express high levels of GFAP by a late time point (10 dpt), similar to the heightened GFAP levels observed clinically.

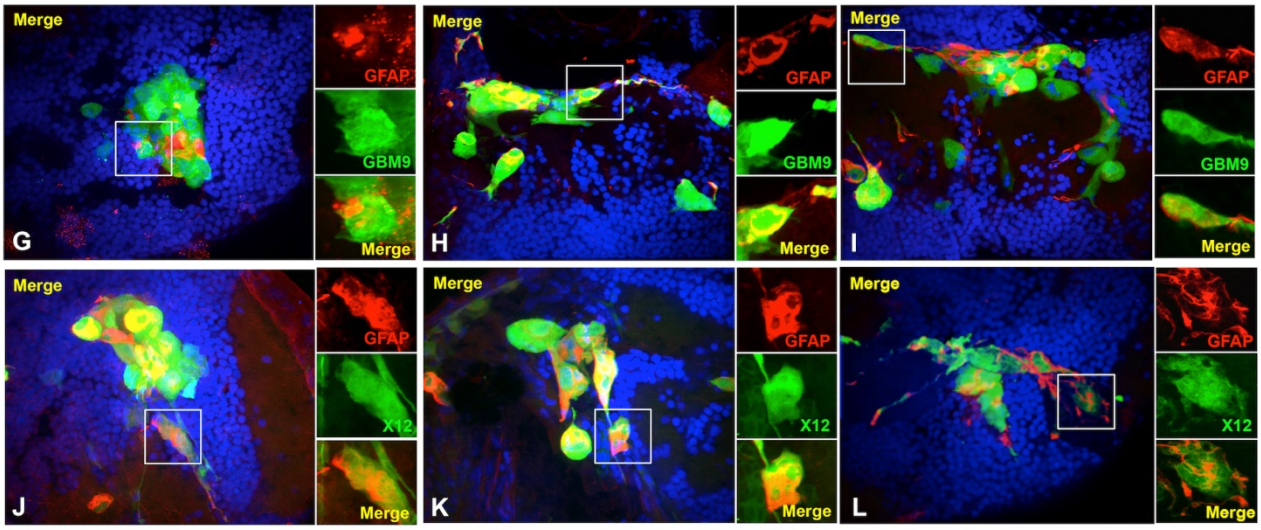

GBM9 neurospheres differentiate over time while X12 adherent cells express high differentiation markers at both early and late time points

Confocal images of GBM9 and X12 on 2 (G, J), 5 (H, K) and 10 (I, L) dpt transverse cryosections. (G-I) GBM9 (green), DAPI (blue) and GFAP (red) at 100×. (J-L) X12 (green), DAPI (blue) and GFAP (red) at 100×. White boxes denote magnified area to the right of the image. *n*=5 animals per group; 30 animals total. Scale bar: 20 μm for main panels and 5 μm for insets.

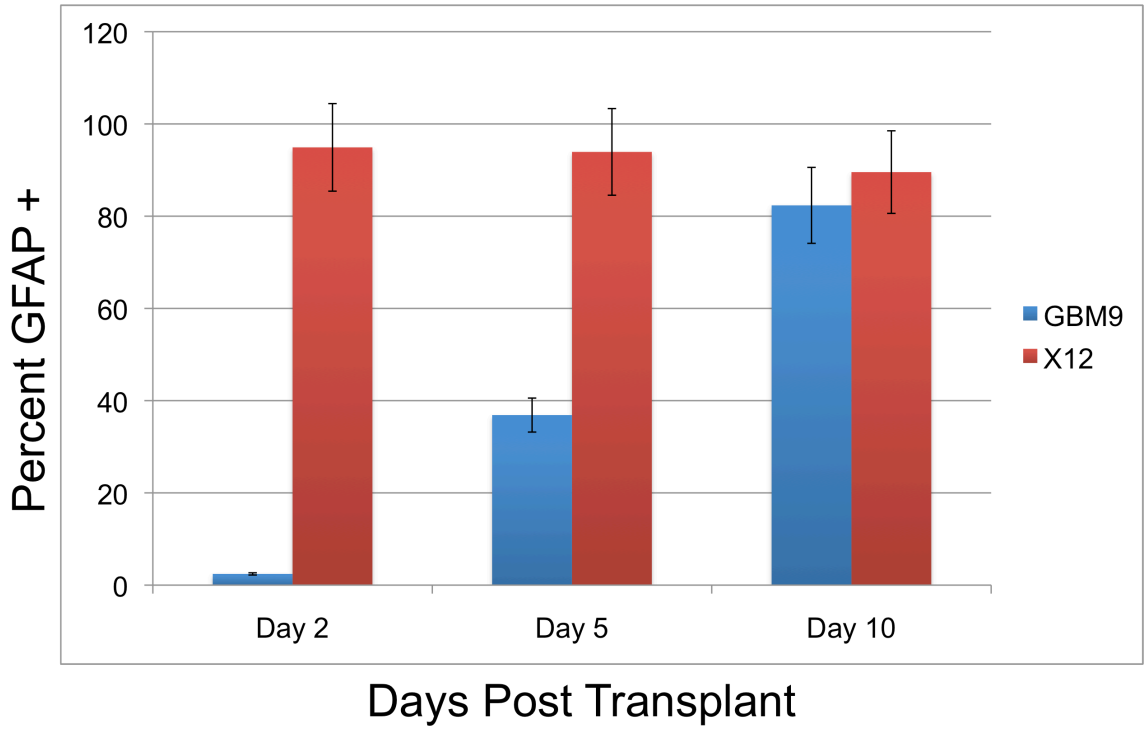

Quantification of the percentage of tumors cells expressing glial fibrillary acidic protein (GFAP) at each time point for GBM9 (blue bar) and X12 (red bar) transplants.

Stem cell populations in GBM9 neurospheres decrease over time while X12 adherent stem cell populations remain constant

The transcription factor Sox-2 was demonstrated to be a marker for cancer stem cells. (Gilbert et al., 2009). Previous mouse model studies have provided evidence that the mutation of normal populations of stem cells is responsible for propagation of glioma growth (Dunn et al, 2012). In a Sox-2 knockdown model, differentiated glioblastoma cells were no longer able to dedifferentiate and thus could not acquire the oncogenic characteristics of a cancer stem cell in a mouse model (Berezovsky et al., 2014). In continuity, another model used an miRNA construct to silence Sox-2 in the tumor-initiating cells of a glioblastoma tumor which resulted in a loss of proliferation and tumor-like phenotype (Gangemi et al., 2009). Thus, there is a mechanistic importance of Sox-2 in the tumorgenicity of glioblastoma. Additionally, Sox-2 expression is extremely limited in healthy cells of an adult human brain, therefore providing clinical relevance through its potential as a therapeutic target (Seymour et al., 2014).

At 2 dpt, we found that roughly 56% of GBM9 neurospheres were positive for Sox-2 expression. Consistent with the dynamic nature of the neurospheres, this expression of Sox-2 decreased over time to ~23% by 10 dpt. The initially high expression rate is in accordance with evidence demonstrated by Annovazzi et al (2011) which showed that neurospheres in culture retain amplified populations of Sox-2 positive cells. Conversely, the number of Sox2+ cells in X12 tumors was roughly 24% at 2 dpt and remained relatively static throughout the 5 and 10 dpt time points. These results suggest that neurospheres retain higher stemness in culture but begin to differentiate when exposed to the microenvironment of the animal brain. They also describe the static nature of stem cell populations in X12 adherent cells.

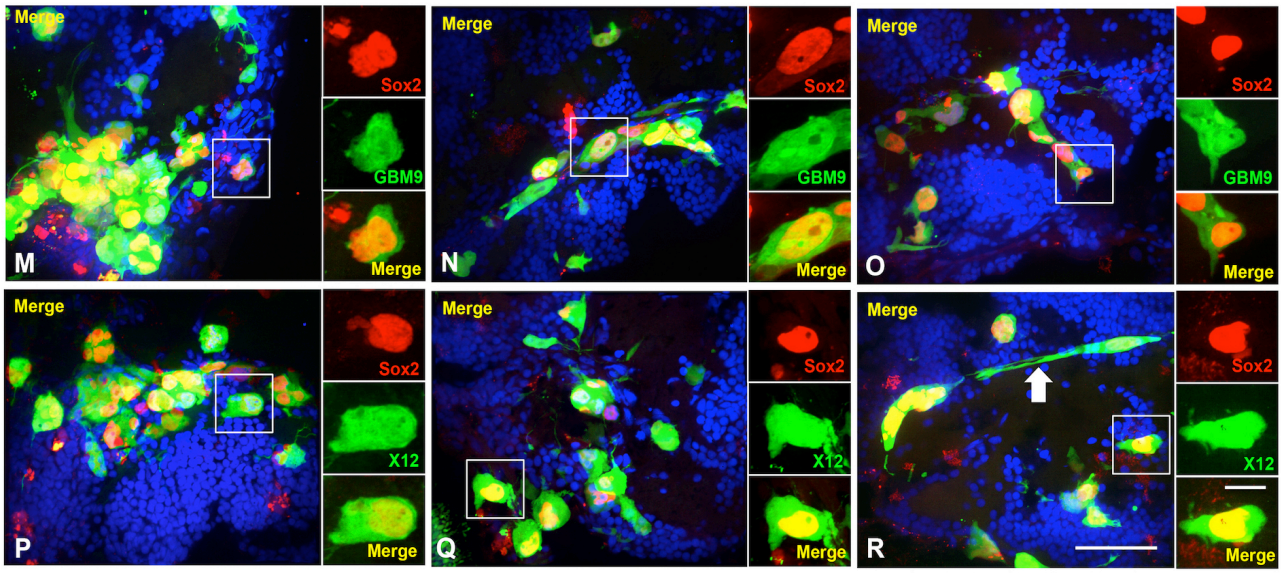

Stem cell populations in GBM9 neurospheres decrease over time while X12 adherent stem cell populations remain constant

Confocal images of GBM9 and X12 on 2 (M,P), 5 (N,Q) and 10 (C,F) dpt transverse cryosections. (O,R) GBM9 (green), DAPI (blue) and Sox2 (red) at 100×. (D-F) X12 (green), DAPI (blue) and Sox2 (red) at 100×. White boxes denote magnified area to the right of the image. *n*=5 animals per group; 30 animals total. Scale bar: 20 µm for main panels and 5 µm for insets.

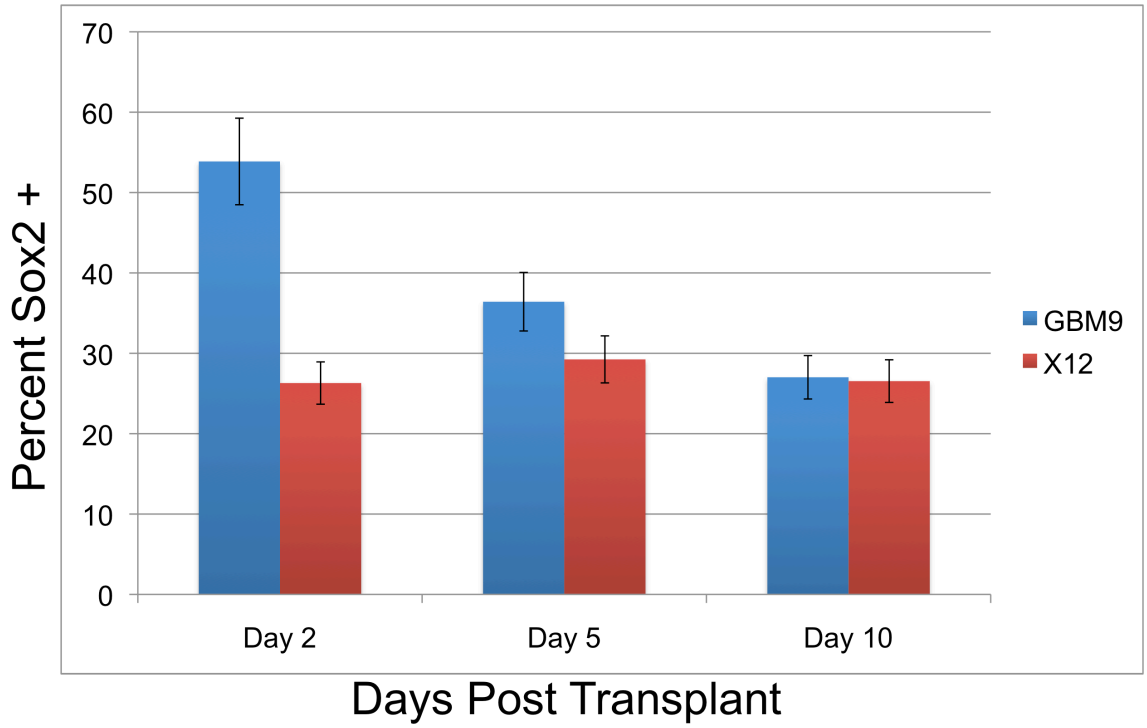

Quantification of the percentage of tumors cells expressing Sox-2 at each time point for GBM9 (blue bar) and X12 (red bar) transplants.

Concurrent immunohistological labeling of multiple markers further characterizes GBM9 neurosphere biology

Following single immunohistological labeling, we wanted to concurrently examine the expression of multiple glioma cell characteristics. To do so, we employed double histological labeling of tumor sections. We utilized primary antibodies with different animal isotypes (mouse and rabbit) and secondary antibodies expressing different wavelengths (594 –red and 405 – blue). For the double labeling, we selected three pairs of expression markers to examine: Ki67 and Vimentin, Ki67 and GFAP, and Proliferating Cell Nuclear Antigen (PCNA) and Sox-2. We chose to only analyze concurrent characteristics of GBM9 neurospheres due to their dynamic nature.

A population of differentiated GBM9 neurospheres is proliferating

To begin, we first examined the relationship between differentiated and dividing cells using a double label of vimentin (differentiation) and Ki67 (proliferation). According to the "Go or Grow" hypothesis of cancer, it is thought that tumor cells may express sets of characteristics which determine two different phenotypes: go (mobile, invasive, metastatic) or grow (stationary, proliferating). In one study, gliomas were observed to upregulate a number of independent genes involved in cell motility upon expressing behavior related to malignant invasion of the environment (Giese et al., 2003). It was also found that glioma cells expressing this invasive phenotype simultaneously experienced decreased proliferation rates and an increased resistance to conventional chemo and radiotherapies (Giese et al., 2003). These results suggest that motile and proliferation characteristics are expressed in tumor cells in an antagonistic manner. On the basis of this hypothesis, we expected to see a demarcation between cells expressing the proliferative marker Ki67 and cells expressing the mesenchymal, differentiation marker

vimentin. However, our previous single labeling data indicated that there may be cells which are expressing both markers of proliferation and differentiation. In the single labeling experiments we found that at 5 dpt, ~40% of neurospheres were expressing Ki67. At the same time point, a different population of neurospheres was ~75% positive for vimentin. Therefore, we wanted to utilize concurrent labeling of these markers to truly examine if overlap existed in the same cell populations.

At 5 dpt, we found that roughly ~40% of GBM9 neurospheres were positive for Ki67, indicating these were proliferating populations. Simultaneously, it was observed that ~75% of neurospheres were positive for vimentin expression, indicating these were mesenchymal, differentiated populations. These numbers are both in accordance with the values we previously observed when individually staining GBM9 cells at 5 dpt. Out of all the GBM9 neurospheres in these sections, ~18% were found to be expressing both vimentin and Ki67. These findings both confirmed and disputed the go or grow hypothesis previously mentioned. A majority of cells expressing the proliferating marker, and thus assumed to be in the “grow” state, were not found to be positive for the differentiated, mesenchymal marker which is indicative of the “go” state. However, the double label confirmed populations of cells that did not exclusively display characteristics for one of these phenotypes, but instead concurrently expressed features of each. These results suggest that although proliferation or differentiation may dictate cell behavior, they are not entirely exclusive in these tumors and cancer cells may exist in a mixed phenotype with both forms of characteristics.

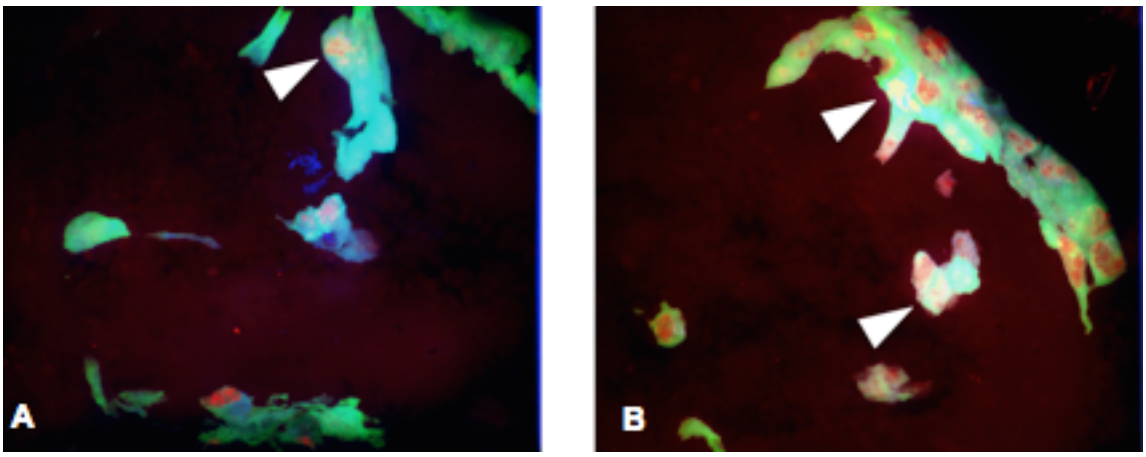

A population of differentiated GBM9 neurospheres is proliferating
Confocal images of GBM9 neurospheres at 5 dpt transverse cryosection (A,B) GBM9 (green), vimentin (blue) Ki67 (red) with triple overlap appearing white at 100×. White arrows denote areas of triple overlap *n*=5 animals

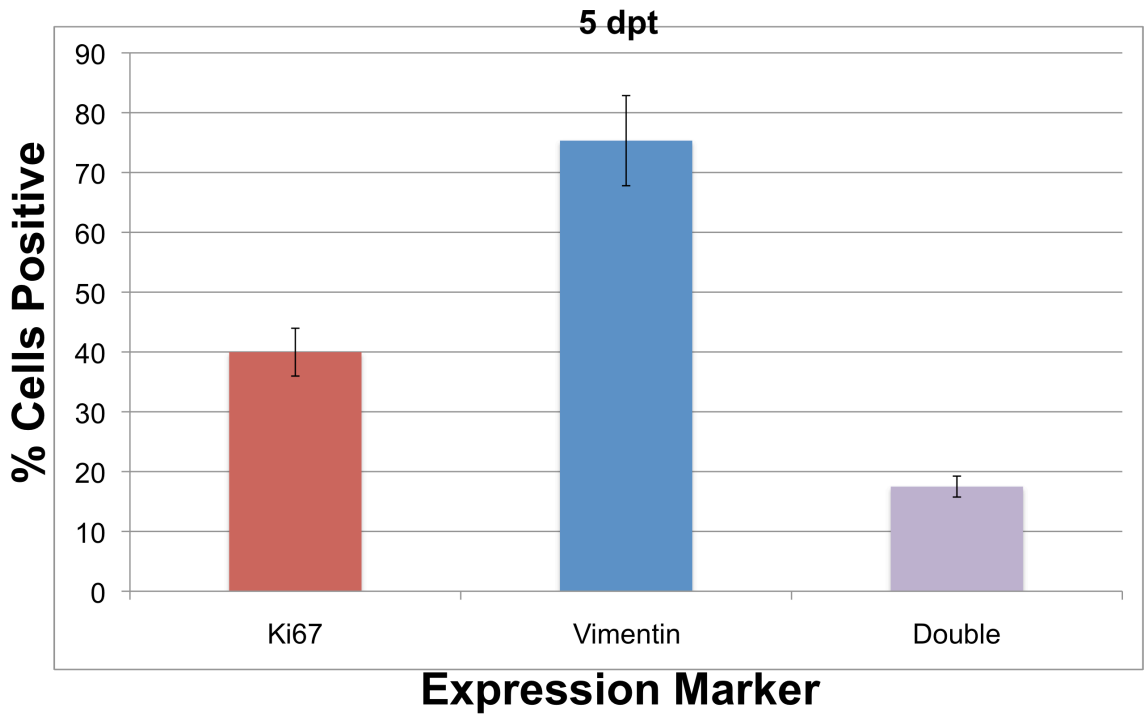

Quantification of the percentage of GBM9 tumors cells expressing Ki67 (red bar), vimentin (blue bar) and both vimentin and Ki67 (purple) at 5 dpt

A majority of GBM9 stem cells are dividing

Next, we investigated the association between proliferation and the presence of stem cells using markers PCNA and Sox-2. PCNA or Proliferating Cell Nuclear Antigen, is a protein involved in the DNA polymerase complex during eukaryotic replication. We selected PCNA as our marker for proliferation, instead of Ki67, based on the specific animal of origin. Both our Ki67 and Sox-2 primary antibodies are derived from rabbit and are the same isotype. Therefore, there would be no way to selectively differentiate secondary antibody binding if these were used in combination. Our PCNA antibody, however, is of mouse origin and can be tagged with an anti-mouse secondary antibody which does not bind to the Sox-2 rabbit antibody. PCNA has often been studied in conjunction with Ki67 as a marker for proliferation in gliomas. Levels of PCNA, as measured by immunohistological staining, were found to be correlated with tumor classification of astrocytomas, with higher PCNA levels correlating with higher grade tumors (Malhan et al., 2010). The results of this study suggested that proliferation levels, as measured by PCNA, were a contributing factor to the level of aggression of astrocytomas (Husain et al., 2010). Additionally, glioblastoma tumors were reported to express the highest levels of PCNA when compared to other types of gliomas such as meningioma, oligodendroglioma, and pilocytic astrocytoma (Kayaselcuk et al., 2002).

We were interested in the relationship between stem cells and proliferation for many reasons. Firstly, current chemotherapeutic agents act by targeting proliferating cells. Tumor recurrence, following treatment, is hypothesized to occur via a subset of quiescent stem cells that were not targeted or were resistant to temozolomide and radiotherapy treatment and which following treatment become highly proliferative. Knockout of this subset of stem-like GBM cells, via TMZ and a targeted ganciclovir administration, halted tumor regrowth and

development (Chen et al., 2012). Therefore, we wanted to examine whether stem cells populations, as labeled by Sox-2, would be dividing prior to treatment and if so, to what degree. This analysis would provide us insight into the ability of current treatments to target these potentially tumor-initiating populations. Based on the idea that GBM tumor formation and development could be directed by undifferentiated neural stem cells, we hypothesized that GBM9 neurospheres would express markers for both stemness (Sox-2) and proliferation (PCNA). In addition, it is hypothesized that GBM may originate from normal populations of cycling and proliferating neural stem cells that become unregulated. In a murine model of glioma, concurrent knockout of the tumor suppressors p53 and Pten contributed to the formation and dedifferentiation of neural stem cells, which ultimately led to the growth of tumors *in vivo* (Zheng et al., 2008). Due to their perceived role in tumor initiation and propagation, we hypothesized that stem cells would be dividing *in vivo*.

At 5 dpt, we found that about ~26% of GBM9 neurospheres were positive for Sox-2 expression. At the same time point, we observed roughly ~37% of PCNA positive neurospheres. The number of Sox-2 expressing cells is generally accordance with the value observed when single labeling GMB9 neurospheres at the 5 dpt time point (~35%). The number of PCNA expressing cells was comparable to the number expressing Ki67 suggesting that they both provide similar metrics of proliferation. The PCNA value was found to be slightly lower than the Ki67 values, likely because PCNA is only active during the synthesis (S) phase of cell replication while Ki67 is active during the G0, G2, and mitosis phases, in addition to the S phase. At 10 dpt, the number of neurospheres expressing PCNA and the number of neurospheres expressing Sox-2 increased to ~45% and to ~28% respectively. Approximately ~19% of neurospheres were found to be simultaneously expressing both Sox-2 and PCNA at 5 pt. At 10

dpt, this number increased to ~26%. The data suggests that a large majority of stem cells, as labeled by Sox-2, are in a proliferating state at this time point. In continuity, about half of all dividing cells are stem cells.

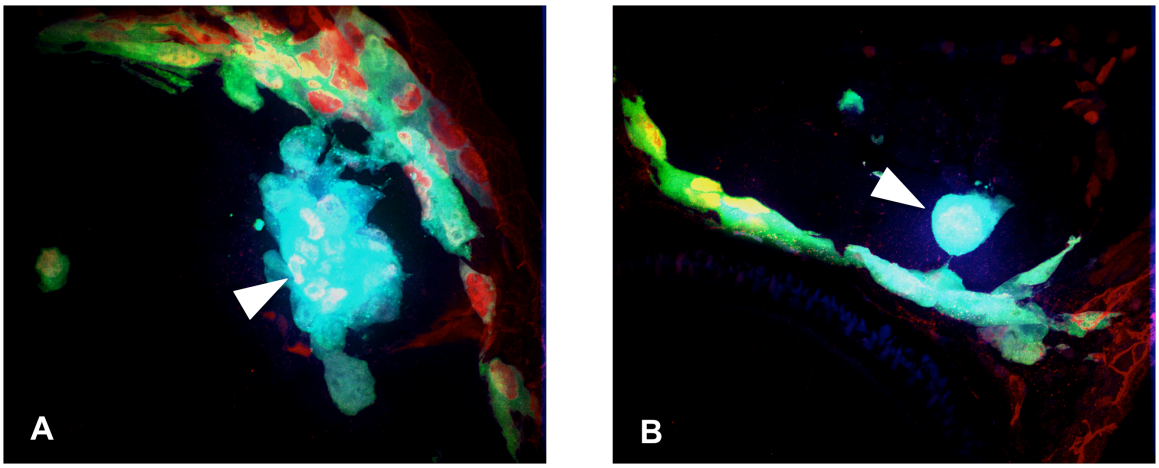

A majority of GBM9 stem cells are dividing
Confocal images of GBM9 neurospheres at 5 dpt transverse cryosection (A,B) GBM9 (green), sox-2 (blue) Ki67 (red) with triple overlap appearing white at 100×. White arrows denote areas of triple overlap *n*=5 animals

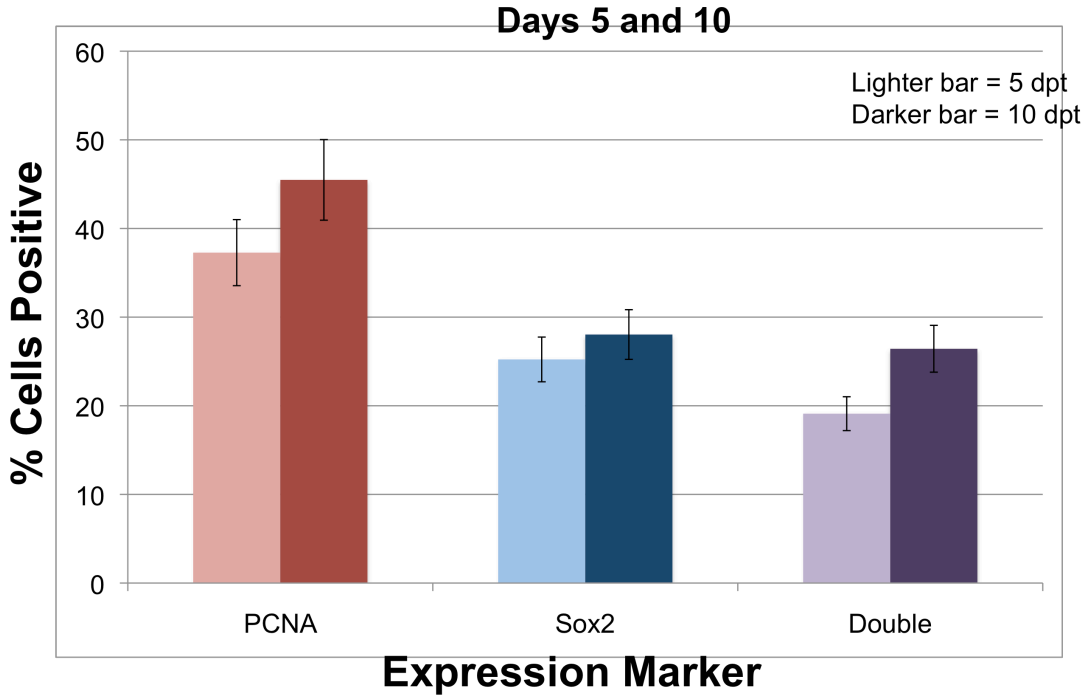

Quantification of the percentage of GBM9 tumors cells expressing PCNA (red bars), Sox2 (blue bars) and both PCNA and Sox2 (purple bars) at 5 dpt (lighter bars; first in sequence) and 10 dpt (darker bars; second in sequence)

A majority of GFAP positive cells are dividing early on but proliferation decreases over time

Finally, we wanted to observe the relationship between proliferation, as measured by Ki67, and GFAP. As previously mentioned, GFAP is known to be a protein expressed in mature glia, such as astrocytes or ependymal cells, making it a marker for differentiation. However, evidence also suggests that certain stem cells or progenitor cells, like radial glia, may express GFAP as well. In order to better understand the cells expressing GFAP in GBM, concurrent characterization of Ki67 and GFAP was performed, specifically to compare the division rates to that of cells expressing vimentin which are presumably differentiated and to that of cells expressing sox-2 which are presumably undifferentiated stem cells. We hypothesized that GFAP positive neurospheres would experience division rates similar to that seen in vimentin positive neurospheres due to the similar expression trends of the two markers we observed during our single labeling experiments.

At 5 dpt, ~36% of GBM9 neurospheres were found to be expressing Ki67. This number increased slightly to ~41% by 10 dpt. At 5 dpt ~47% of cells were positive for GFAP expression and this number increased significantly to 84% at 10 dpt. These values were consistent with those observed during the double labeling experiments. It was found that at 5 dpt ~29% of neurospheres were positive for both Ki67 and GFAP expression. This population decreased to ~12% by 10 dpt. These data suggests that at an earlier time point, the division rates of GFAP positive cells are more comparable to that of Sox-2 positive cells. Although the number of cells expressing GFAP increases significantly, the division rate decreases by 10 dpt to a level similar to that of vimentin positive cells.

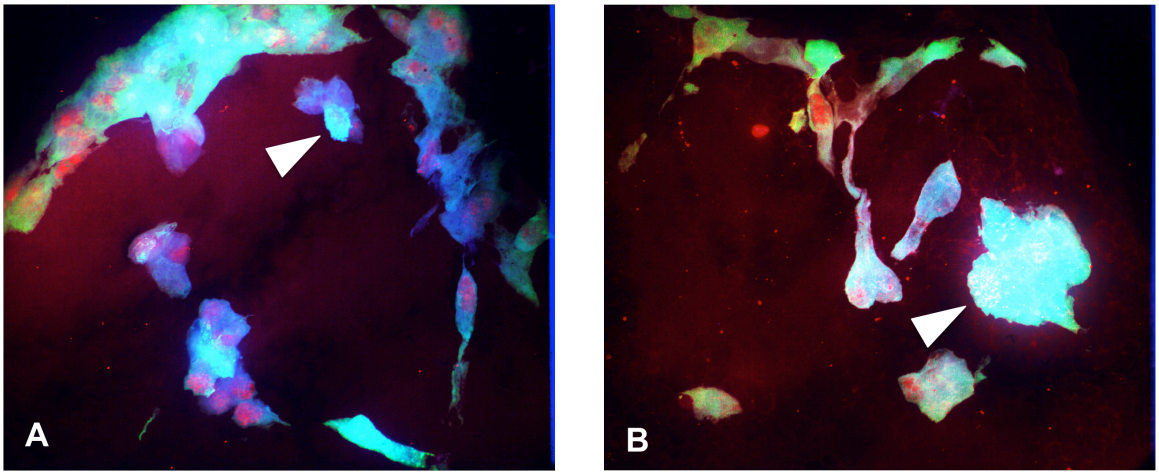

A majority of GFAP positive cells are dividing early on but proliferation decreases over time
Confocal images of GBM9 neurospheres at 5 dpt transverse cryosection (A,B) GBM9 (green), GFAP (blue) Ki67 (red) with triple overlap appearing white at 100×. White arrows denote areas of triple overlap *n*=5 animals

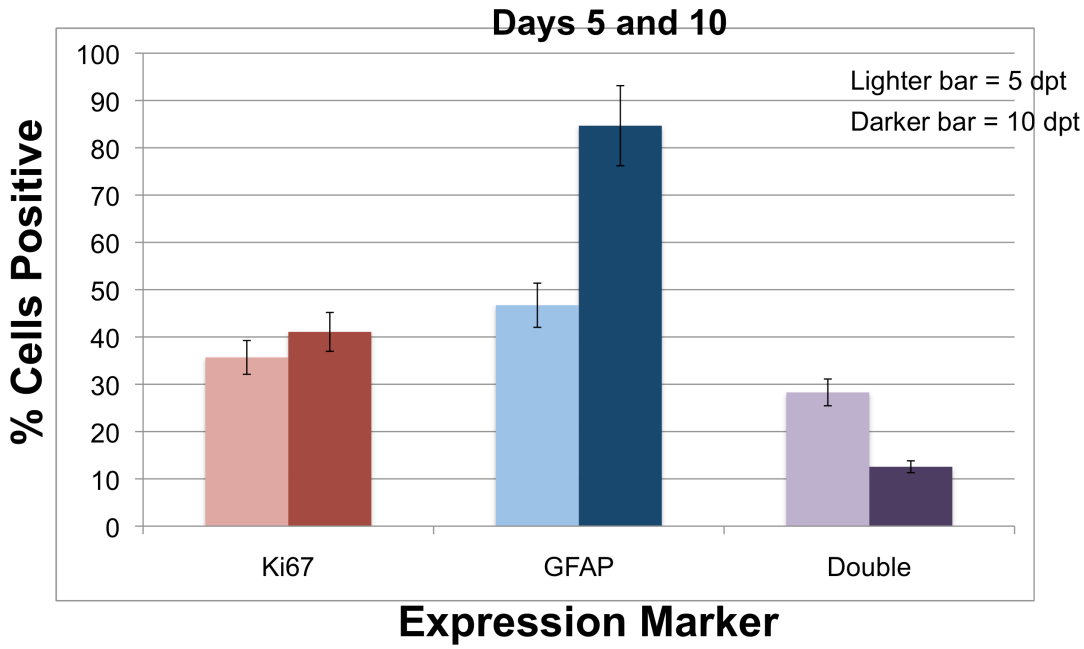

Quantification of the percentage of GBM9 tumors cells expressing Ki67 (red bars), GFAP (blue bars) and both Ki67 and GFAP (purple bars) at 5 dpt (lighter bars; first in sequence) and 10 dpt (darker bars; second in sequence)

Discussion

Here we have shown the immunohistological characterization of tumors in a novel xenotransplantation model of glioblastoma in zebrafish. This characterization provides us a deeper understanding of GBM in this animal model and provides a measure of validity in comparison to human tumors, thereby increasing the model's future potential for studying the biology of GBM and for drug screens.

Our comparison of adherent cell and neurosphere GBM populations provides insight into the utilization of these cell types in research. We have demonstrated that although both cell types exhibit markers used to characterize patient tumors, the levels and expression patterns vary between adherent cells and neurospheres. As our preliminary data suggested, both cell types were dividing. However, we were surprised to find that X12 adherent cells displayed higher levels of proliferation when compared to the GBM9 neurospheres. Prior to immunohistological characterization, our lab analyzed the survival time of animals transplanted with X12 cells and GBM9 neurospheres. It was found that GBM9 neurospheres exhibited greater lethality in animals when compared to similar cell burden transplants of X12 adherent cells. In fact, smaller burdens (51-90 cells) of transplanted GBM9 neurospheres were more lethal than larger burdens of transplanted X12 adherent cells (91-140). Due to the observed greater lethality, we expected neurospheres to exhibit higher division rates. Our findings suggest that general levels of cell division may not be directly indicative of the behavior or aggressiveness of GBM tumors *in vivo*. One possibility is that the percentage of stem cells is more indicative of aggressive tumors.

Beyond differences in cell division, we also observed variability in the expression of differentiation and stem cell markers. The X12 adherent cells displayed relatively constant levels of vimentin, GFAP, and Sox-2 with a high number of cells expressing vimentin and GFAP and a

low number of cells expressing Sox-2. These levels of expression are congruent with *in vitro* data which suggests that adherent cells are highly differentiated in serum containing media and are composed of a less diverse cell population. In addition, this characterization highlighted the static nature of these adherent cells *in vivo*, with little change seen in the expression of these different characteristics at various time points. Conversely, GBM9 neurospheres experienced diverse expression of markers at these time points. At an early time point, levels of both GFAP and vimentin expression were low, suggesting that neurospheres are generally undifferentiated *in vitro*. The levels of both markers increase at both 5 and 10 day time points suggesting that the tumor cells are differentiating when exposed to the microenvironment of the brain *in vivo*. In contrast, Sox-2 expression, a marker of stem cells, began high and decreased over time. This decline suggests that stem cells are differentiating over time which is in accordance with the increase of vimentin and GFAP over time. The higher initial population of stem cells in neurospheres may be a contributing factor to their greater lethality *in vivo* when compared to X12 adherent cells. In addition, the high levels of stem cell populations and low levels of differentiated populations at an early time point are in agreement with *in vitro* data that neurospheres retain higher levels of stemness and a more variable cell population in culture. Due to the dynamic nature of GBM9 neurospheres *in vivo*, particularly when compared to X12 adherent cells, we find them to be a more accurate recapitulation of human glioblastoma in our animal model.

To further investigate how certain cell populations were behaving *in vivo*, we performed concurrent immunohistological characterization of markers in GBM9 neurospheres. The double label of Ki67 and vimentin revealed that expression of these markers is not entirely exclusive as originally hypothesized. The go or grow theory of cancer suggests that tumor cells exhibit either

a motile, mesenchymal “go” phenotype or a stationary, proliferative “grow” phenotype. However, our results demonstrate that there is a population of cells simultaneously expressing markers indicative of both growth and mesenchymal motility. These results may reflect a difference of glioblastoma cell behavior from other types of cancers that this theory characterizes. These findings also attest to the deviation and heterogeneity of cancer cell expression. For example, we normally think of unphosphorylated vimentin in non-dividing cells. However, cancer cells are, by nature, unregulated and may express proteins that are normally not expressed concurrently, thus reflecting their aberrant nature. The concurrent labeling of PCNA and Sox-2 revealed that a majority of GBM9 stem cells are dividing. These dividing stem cells of are thought to be responsible for tumor propagation (Lathia et al., 2015). Specifically, this high population of dividing stem cells may help explain the increased lethality observed in the GBM9 neurospheres. From 5 to 10 dpt, the number of stem cells dividing increased by a value that cannot solely be explained by a concomitant increase in the number of overall stem cells. This increase suggests that even a later time point, GBM9 neurospheres are retaining active populations of stem cells which may continue to propagate the tumor. Interestingly, populations of Ki67 negative stem cells were also present, although low in number. It is believed that non-dividing or quiescent stem cells, such as these, may be responsible for tumor recurrence following treatment with therapeutics like temozolomide which specifically target dividing cells (Lathia et al., 2015). Finally, examined populations of cells expressing both Ki67 and GFAP. Interestingly, a majority of GFAP positive cells were dividing at 5 dpt. This value was higher than that of dividing vimentin cells or of dividing sox-2 cells, suggesting that in GBM GFAP may be expressed in both differentiated cells and stem cells. The number of dividing GFAP positive cells decreased at 10 dpt, opposite of the level of dividing Sox-2 positive cells. This

opposing relationship demonstrates that although the overall level of proliferating cells remained constant in GBM9 neurospheres, the division rates of particular cell populations changed over time. These findings further support our conclusion of the dynamic nature of the GBM9 neurospheres.

In the future, we would like to further understand the relationship between GFAP and stem cells via a GFAP and Sox-2 concurrent label. Additionally, we are interested in investigating how tumor biology changes following treatment with chemotherapeutic agent temozolomide. To test this, we plan to treat animals with a 5 day dosage of temozolomide, comparable to the human treatment timeline, and then perform immunohistological characterization of the markers used in this paper to understand if they change following treatment.

Overall, we have concluded that glioblastoma tumors xenotransplanted into zebrafish following this methodology exhibit markers that resemble those expressed in human patient tumors. Additionally, we have found GBM9 neurospheres to be a more dynamic cell type, more closely resembling the characteristics of patient tumors when compared to X12 adherent cells. Finally, we observed that although the overall proliferation levels of GBM9 neurospheres did not change over time, specific cell populations varied in their rates of division at different observed time points.

Material and Methods

Cell Culture (Cited directly from Welker et al., 2016)

GBM9 and X12 cells were obtained from tumor specimens as previously described and modified with GFP to generate GBM9-GFP and X12-v2 (Williams et al., 2011; Godlewski et al.,

2008; Wojton et al., 2014;Giannini, 2005). Neurospheres (GBM9, mNSC) were kept in Neurobasal Media (Gibco, Grand Island, NY, USA) supplemented with B-27, GlutaMax (Gibco) and growth factors EGF and FGF (R&D Systems, Minneapolis, MN, USA) in flasks (Corning Inc., Corning, NY, USA). Adherent cells (X12-v2) were kept in Dulbecco's modified Eagle's medium (Gibco) and 10% fetal bovine serum for the first week in culture and then in 2% fetal bovine serum for the duration of experiments (GE Healthcare, Logan, UT, USA) in culture dishes (Corning Inc.). Cells were tested for mycoplasma by PCR every 8-12 weeks (GBM9 neurospheres) or 6 months (X12 cells). Both lines were GFP labeled and are referred to throughout this work as GBM9 and X12.

Zebrafish lines (Cited directly from Welker et al., 2016)

Zebrafish were maintained at 28°C unless otherwise noted. AB×Tupfel long fin (ABLF) animals are referred to as wild type. *casper* mutants (*roy*;*nacre*; White et al., 2008) were obtained from Dr Leonard Zon's laboratory at Children's Hospital Boston. All animals were kept in accordance with The Ohio State University Institutional Animal Care and Use Committee protocols. For all experiments, animals were obtained from group crosses.

Transplants (Cited directly from Welker et al., 2016)

For transplantation, X12 cells were grown to 70-80% confluence then washed twice with PBS (Gibco), trypsinized (Gibco), dissociated, counted, and resuspended in Hank's balanced salt solution (HBSS; Gibco). When GBM9 neurospheres reached ∼1 mm diameter they were dissociated using TrypLE (Gibco). GBM9 cells were counted and resuspended in HBSS (Gibco) within 15 min of transplantation. GFP-labeled mNSC cells were obtained from Dr Jaime Imitola's laboratory and counted for control experiments. Cells were transplanted in the vicinity of the midbrain-hindbrain boundary of 36 hpf tricaine-anesthetized embryos (Sigma-Aldrich, St

Louis, MO, USA) using a back-loaded pulled borosilicate glass needle (Sutter Instruments, Novato, CA, USA) and avoiding the ventricle. Sham-injected animals received an injection of 1-2 nl of HBSS into the midbrain. After transplantation, animals were allowed to recover in fish water and 100 units penicillin/100 µg streptomycin/ml (Invitrogen, Grand Island, NY, USA) in 24-well plates (Corning Inc.) on a warming plate at 32°C. For tumor cell engraftment, animals were screened at 24 h post-transplantation (hpt) and, based on cell counts, fell into one of the following four groups: (i) 10-25 cells; (ii) 26-50 cells; (iii) 51-90 cells; or (iv) 91-140 cells. Animals were then tracked for survival. After the optimal cell number was established, larvae were screened at 24 hpt for ∼50 cells for GBM9 and ∼100 cells for X12 per animal. Animals without the optimal number of cells were screened out of the study. SPSS (Statistical Package for the Social Sciences; IBM Corp., Armonk, NY, USA) was used to create Kaplan–Meier survival curves and to calculate median survival. Animals were fed, beginning at 6 dpf, using standard larval food. Small amounts of food were added to each 24-well plate and rinsed out after 30 min with fresh fish water. Experiments consisted of animals obtained from multiple group crosses (usually three females and two males) and cells obtained from the same passage. Animals was obtained from between two and four experiments consisting of ∼24 transplants per experiment. Details on numbers of animals are provided in the figure legends.

Cryostat Sections

Casper animals transplanted with GBM9 cells were fixed at 5 or 10 dpt with 4% paraformaldehyde (PFA; Sigma-Aldrich) in PBS (Sigma-Aldrich) at 4°C. Animals were fixed for a minimum of 24 hours in order to compensate for the softness of tumor cells in comparison to the animal brain tissue. The animals were then transferred into 30% sucrose in PBS (Thermo-Fisher Scientific, Waltham, MA, USA) at 4°C overnight. Next, animals were placed in

individual silicon molds filled with OCT compound (Sakura Finetek, Torrance, CA, USA) and were frozen at -80°C for 15 minutes. Frozen animals were cut into 20 micron sections using a cryostat machine. Sections were deposited onto Super Frost Plus slides (Thermo-Fisher Scientific). Sections were cut in the transverse plane, comparable to the coronal sections used in mouse and human brains. Slides were stored at 4°C overnight and subsequently used for histological staining.

Histology and Immunohistochemistry

All staining was performed on prepared slides of 20 micron animal sections. Primary antibodies were diluted in either 3% or 5% bovine serum albumin in PBS and incubated at 4°C overnight. Secondary antibodies were diluted in 1% Triton in PBS and incubated at room temperature for 2 hours.

Ki67

Following cryosection, slides were initially outlined with a Dako Pen (Dako, Carpinteria, CA, USA). Slides were washed 3 times in PBS, 10 minutes per wash for a total of 30 minutes and then permeabilized with 0.5% Triton (Thermo-Fisher Scientific) for 10 minutes. Slides were returned to a 10 minutes PBS wash before antigen retrieval. For antigen retrieval, slides were placed in two, 7 minute rounds of boiling PBS for a total of 14 minutes. Following retrieval, slides were washed in fresh PBS. Slides were blocked for one hour in 3% or 5% bovine serum albumin in PBS (Jackson ImmunoResearch, West Grove, PA, USA) and were then stained with anti-Ki67 (D3B5) rabbit antibody at a 1/100 concentration (Cell Signaling, Danvers, MA, USA; 91295) overnight at 4°C. The following day, slides were washed in three, 30 minute rounds of PBS for a total of 90 minutes. Slides were permeabilized with 0.1% Triton for 10 minutes before being switched into secondary antibody (Life Technologies, Carlsbad, CA, USA) Alexa-Fluor

594 goat anti-rabbit IgG at 1:300 concentration for 2 hours at room temperature. Finally, slides were washed with 3 rounds of PBS, 20 minutes each round, for a total of 60 minutes and then mounted in Fluoromount with 4', 6-diamidino-2-phenylindole dihydrochloride (DAPI; Sigma-Aldrich) and coverslipped (Thermo-Fisher Scientific).

Vimentin

Procedure was the same as Ki67 except without antigen retrieval. However, in double labeling combinations with nuclear proteins, antigen retrieval was performed as an inevitable part of the procedure. The primary antibody was monoclonal vimentin antibody at a 1:200 concentration. (mouse clone V9; Dako; M0725). The secondary antibodies used were Alexa-Fluor 594 rabbit anti-mouse IgG at a 1:200 concentration. (Life Technologies) or Alexa-Fluor 405 goat anti-mouse IgG (Life Technologies) at a 1:200 concentration. The 594 secondary was used for the single labeling experiments. The secondary antibody used for double labeling experiments was dependent on the wavelength of the other antibody in the label.

Sox-2

Procedure was the same as Ki67 with antigen retrieval. The primary antibody used was polyclonal rabbit anti-Sox2 antibody at a 1:50 concentration (Abcam, Cambridge, MA, USA; ab97959). The secondary antibody used for the single labeling with DAPI was Alexa-Fluor 594 goat anti-rabbit IgG at a 1:200 concentration, as above. The secondary antibody used for the double labeling was Alexa-Fluor 405 goat anti-rabbit IgG (Life Technologies) at a 1:200 concentration.

Glial Fibrillary Acidic Protein (GFAP)

Procedure was the same as Ki67 except without antigen retrieval. However, in double labeling combinations with nuclear proteins, antigen retrieval was performed as an inevitable

part of the procedure. The primary antibodies used were polyclonal rabbit anti-glial fibrillary acidic protein at a 1:200 concentration (GFAP, Dako; Z0334) or monoclonal mouse anti-glial fibrillary acidic protein at a 1:100 concentration (GFAP, DAKO; M0761). The primary antibody used was dependent on the animal origin of the other antibody in the double label. The secondary antibodies used were Alexa-Fluor 594 goat anti-rabbit IgG at a 1:200 concentration, as above, and Alexa-Fluor 405 goat anti-mouse IgG at a 1:200 concentration. The secondary antibody used was dependent on the animal origin of the primary antibody.

Proliferating Cell Nuclear Antigen (PCNA)

Procedure was the same as Ki67 with antigen retrieval. The primary antibody used was proliferating cell nuclear antigen at a 1:100 concentration. (PCNA, DAKO; M0879) and the secondary antibody used was Alexa-Fluor 594 goat anti-mouse IgG at a 1:200 concentration.

Imaging

Imaging of immunohistochemistry and staining analysis was performed on the Andor spinning disk confocal microscope (Andor, Oxford, UK;). 0.4 micron Z-stacks were created from individual 20 micron sections and were observed through three filter channels: 405 (blue; immunohistochemistry), 488 (green; tumor cells), and 594 (red; immunohistochemistry). Cell count and staining analysis was performed on these imaged Z-stacks. The total number of cells was counted, identifiable by green fluorescent expression, followed by the number of cells expressing each individual histological stain. Finally, the number of cells expressing both histological stains was evaluated. To create the triple labeled images, the Z-stacks were compressed in all three filter channels.

References

Annovazzi, L., Mellai, M., Caldera, V., Valente, G. & Schiffer, D. SOX2 expression and amplification in gliomas and glioma cell lines. *Cancer Genomics Proteomics* **8,** 139–47 (2011).

Berezovsky, A. D. *et al.* Sox2 promotes malignancy in glioblastoma by regulating plasticity and astrocytic differentiation. *Neoplasia* **16,** 193–206, 206.e19–25 (2014).

Chen, J. *et al.* A restricted cell population propagates glioblastoma growth after chemotherapy. *Nature* **488,**522–6 (2012).

Dinca, E. B. *et al.* Bioluminescence monitoring of intracranial glioblastoma xenograft: response to primary and salvage temozolomide therapy. *J. Neurosurg.* **107,** 610–6 (2007).

Dooley, K. & Zon, L. I. Zebrafish: a model system for the study of human disease. *Curr. Opin. Genet. Dev.* **10,** 252–6 (2000).

Feitsma, H. & Cuppen, E. Zebrafish as a cancer model. *Mol. Cancer Res.* **6,** 685–94 (2008).

Fortin, S. *et al.* Galectin-1 is implicated in the protein kinase C epsilon/vimentin-controlled trafficking of integrin-beta1 in glioblastoma cells.*Brain Pathol.* **20,** 39–49 (2010).

Gangemi, R. M. *et al.* SOX2 silencing in glioblastoma tumor-initiating cells causes stop of proliferation and loss of tumorigenicity. *Stem Cells* **27,** 40–8 (2009).

Giannini C. (2005). Patient tumor EGFR and PDGFRA gene amplifications retained in an invasive intracranial xenograft model of glioblastoma multiforme. *Neuro Oncol.* 7, 164-176. 10.1215/S1152851704000821

Giese, A., Bjerkvig, R., Berens, M. E. & Westphal, M. Cost of migration: invasion of malignant gliomas and implications for treatment. *J. Clin. Oncol.* **21,** 1624–36 (2003).

Gilbert, C. A. & Ross, A. H. Cancer stem cells: cell culture, markers, and targets for new therapies. *J. Cell. Biochem.* **108,** 1031–8 (2009).

Glioblastoma (GBM). (n.d.). Retrieved April 30, 2016, from http://www.abta.org/brain-tumor-information/types-of-tumors/glioblastoma.html?referrer=httpps://www.google.com

Godlewski J., Nowicki M. O., Bronisz A., Williams S., Otsuki A., Nuovo G., Raychaudhury A., Newton H. B., Chiocca E. A. and Lawler S. (2008). Targeting of the Bmi-1 oncogene/stem cell renewal factor by microRNA-128 inhibits glioma proliferation and self-renewal. *Cancer Res.* 68, 9125-9130. 10.1158/0008-5472.CAN-08-2629

Guichet, P.-O. O. *et al.* Asymmetric Distribution of GFAP in Glioma Multipotent Cells. *PLoS ONE* **11,**e0151274 (2016).

Jakovlevs, A. *et al*. Heterogeneity of Ki-67 and p53 Expression in Glioblastoma : Acta Chirurgica Latviensis. *De Gruyter*. **14,** 3-45 (2014)

Jung *et al.* Serum GFAP is a diagnostic marker for glioblastoma multiforme.*Brain* **130,** 3336–3341 (2007).

Kayaselçuk, F., Zorludemir, S., Gümürdühü, D., Zeren, H. & Erman, T. PCNA and Ki-67 in central nervous system tumors: correlation with the histological type and grade. *J. Neurooncol.* **57,** 115–21 (2002).

Kitambi, S. S. *et al.* Vulnerability of glioblastoma cells to catastrophic vacuolization and death induced by a small molecule. *Cell* **157,** 313–28 (2014).

Lal, S., La Du, J., Tanguay, R. L. & Greenwood, J. A. Calpain 2 is required for the invasion of glioblastoma cells in the zebrafish brain microenvironment.*J. Neurosci. Res.* **90,** 769–81 (2012).

Lathia, J. D., Mack, S. C., Mulkearns-Hubert, E. E., Valentim, C. L. L. & Rich, J. N. Cancer stem cells in glioblastoma. *Genes Dev*. **29,**1203–17 (2015).

Malhan, P., Husain, N., Bhalla, S., Gupta, R. K. & Husain, M. Proliferating cell nuclear antigen, p53 and micro vessel density: Grade II vs. Grade III astrocytoma. *Indian J Pathol Microbiol* **53,** 20–3 (2010).

Ostrom, Q. T. *et al.* CBTRUS statistical report: primary brain and central nervous system tumors diagnosed in the United States in 2007-2011. *Neuro-oncology* **16 Suppl 4,** iv1–63 (2014).

Peal, D. S., Peterson, R. T. & Milan, D. Small molecule screening in zebrafish. *J Cardiovasc Transl Res* **3,** 454–60 (2010).

Rahman, M. *et al.* Neurosphere and adherent culture conditions are equivalent for malignant glioma stem cell lines. *Anat Cell Biol* **48,** 25–35 (2015).

Richmond, A. & Su, Y. Mouse xenograft models vs GEM models for human cancer therapeutics. *Dis Model Mech* **1,** 78–82 (2008).

Satelli, A. & Li, S. Vimentin in cancer and its potential as a molecular target for cancer therapy. *Cell. Mol. Life Sci.***68,** 3033–46 (2011).

Schröder, R., Feisel, K. D. & Ernestus, R.-I. I. Ki-67 labeling is correlated with the time to recurrence in primary glioblastomas. *J. Neurooncol.* **56,** 127–32 (2002).

Seymour, T., Nowak, A. & Kakulas, F. Targeting Aggressive Cancer Stem Cells in Glioblastoma. *Front Oncol* **5,** 159 (2015).

Stupp, R. *et al.* Effects of radiotherapy with concomitant and adjuvant temozolomide versus radiotherapy alone on survival in glioblastoma in a randomised phase III study: 5-year analysis of the EORTC-NCIC trial.*Lancet Oncol.* **10,** 459–66 (2009).

Trog, D., Yeghiazaryan, K., Schild, H. H. & Golubnitschaja, O. Up-regulation of vimentin expression in low-density malignant glioma cells as immediate and late effects under irradiation and temozolomide treatment. *Amino Acids***34,** 539–45 (2008).

Vittori, M., Motaln, H. & Turnšek, T. L. The study of glioma by xenotransplantation in zebrafish early life stages. *J. Histochem. Cytochem.* **63,**749–61 (2015).

Welker, A. M. *et al.* Standardized orthotopic xenografts in zebrafish reveal glioma cell-line-specific characteristics and tumor cell heterogeneity. *Dis Model Mech* **9,** 199–210 (2016).

White R., Rose K. and Zon L. (2013). Zebrafish cancer: the state of the art and the path forward. *Nat. Rev. Cancer* 13, 624-636. 10.1038/nrc3589

Williams S. P., Nowicki M. O., Liu F., Press R., Godlewski J., Abdel-Rasoul M., Kaur B., Fernandez S. A., Chiocca E. A. and Lawler S. E. (2011). Indirubins decrease glioma invasion by blocking migratory phenotypes in both the tumor and stromal endothelial cell compartments. *Cancer Res.* 71, 5374-5380. 10.1158/0008-5472.CAN-10-3026

Wojton J., Meisen W. H., Jacob N. K., Thorne A. H., Hardcastle J., Denton N., Chu Z., Dmitrieva N., Marsh R., Van Meir E. G. et al. (2014). SapC-DOPS-induced lysosomal cell death synergizes with TMZ in glioblastoma. *Oncotarget* 5, 9703-9709. 10.18632/oncotarget.2232

Yang, X. J. *et al.* TGF-β1 enhances tumor-induced angiogenesis via JNK pathway and macrophage infiltration in an improved zebrafish embryo/xenograft glioma model. *Int. Immunopharmacol.* **15,** 191–8 (2013).

Zheng, H. *et al.* Pten and p53 converge on c-Myc to control differentiation, self-renewal, and transformation of normal and neoplastic stem cells in glioblastoma. *Cold Spring Harb. Symp. Quant. Biol.* **73,** 427–37 (2008).